INTERNATIONAL JOURNAL OF ROBUST AND NONLINEAR CONTROL
Int. J. Robust Nonlinear Control 2006; **16**:467–483
Published online 2 May 2006 in Wiley InterScience (www.interscience.wiley.com). DOI: 10.1002/rnc.1070

A two-degree-of-freedom $\mathscr{H}_\infty$ control design method for robust model matching

Arvin Dehghani[1,2,*,†], Alexander Lanzon[1,2] and Brian D. O. Anderson[1,2]

[1] *Department of Information Engineering, Research School of Information Sciences & Engineering, The Australian National University, Canberra, ACT 0200, Australia*
[2] *National ICT Australia Ltd., Locked Bag 8001, Canberra, ACT 2601, Australia*

SUMMARY

We propose an $\mathscr{H}_\infty$ controller design method which achieves a closed-loop transfer function equal or otherwise sensibly close to a desired transfer function, viz. a model reference design. The proposed controller design method inherits the model reference feature of the internal model control design method and incorporates the weighting scheme of the $\mathscr{H}_\infty$ loop-shaping. It utilizes Youla–Kucera parameterization in a two-degree-of-freedom scheme to achieve robust model reference and high performance design while ensuring a sensible robust stability margin, and can be readily applied to the generic class of LTI systems (SISO, MIMO, stable, unstable). Copyright © 2006 John Wiley & Sons, Ltd.

KEY WORDS: robust control; internal model control; adaptive control

1. INTRODUCTION

In many applications, control objectives include achieving direct control over the closed-loop bandwidth and the transfer function from reference to plant output, where the ultimate goal is to shape the magnitude of the transfer function T_{yr} in Figure 1. Parameterization of all stabilizing controllers of a plant in terms of the set of all stable proper transfer functions [1–3] results in a T_{yr} which is affine in the parameterizing transfer function, as reviewed in Section 2.1. For stable plants, this parameterization becomes simpler and is sometimes known as internal model control (IMC) [4], and in principle allows—for stable plants with no jω-axis zeros—the design of a controller that achieves a closed-loop magnitude response exactly equal to that of a desired transfer function known as the IMC filter F (see Section 2.2) containing a free parameter tuning the closed-loop bandwidth.

*Correspondence to: Arvin Dehghani, Department of Information Engineering, Research School of Information Sciences & Engineering, The Australian National University, Canberra, ACT 0200, Australia.
†E-mail: arvin.dehghani@anu.edu.au

Contract/grant sponsor: ARC Discovery; contract/grant number: DP0342683
Contract/grant sponsor: National ICT Australia

Received 3 April 2005
Revised 7 July 2005
Accepted 27 January 2006

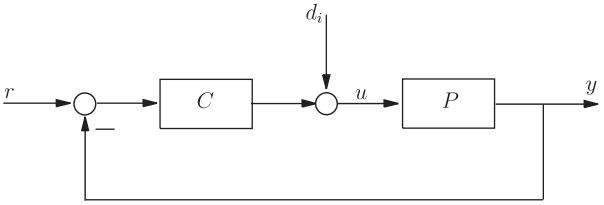

Figure 1. Standard feedback configuration.

This important bonus of offering instantaneous and direct tuning of the bandwidth of T_{yr} in Figure 1 via setting the bandwidth of F is utilized in the area of adaptive robust control to progressively increase the closed-loop bandwidth in identification and controller re-design [5, 6]. Nonetheless, the IMC design method is restrictive and may result in a design which is unacceptable on various practical fronts [7]. The IMC design method even has to be almost abandoned when the plant is unstable since the design method becomes much more involved, to say the least, and there are a set of interpolation constraints to satisfy (Section 2.3). Even worse is that the above-mentioned single design parameter no longer directly tunes the closed-loop bandwidth, see Section 2.3 and References [4, 8]. Research directed at finding ways round the above-mentioned difficulties has resulted in design methods which are often application-specific (e.g. excluding unstable plants with unstable zeros) [8, 9], rather than generic.

Even for stable plants, there are circumstances where the IMC design method can result in undesirable or even unacceptable design which are detailed in References [7, 10] and outlined in Section 2.4. The related disadvantages of the IMC design method are partly due to the fact that the design method deals specifically with the complementary sensitivity, viz. $T_{yr} = P(I + PC)^{-1}C$ in Figure 1, by setting its magnitude response (Section 2.2), but it does not explicitly handle the other transfer functions ($T_{yd_i}, T_{ur}, T_{ud_i}$) and hence it may fail to ensure that their magnitudes are acceptable. However, these three transfer functions do relate to certain properties of a feedback loop [11] as discussed in Section 2.4.

The aforementioned difficulties are also partly related to the associated design method which has a *single* degree of freedom expressed in terms of a single Youla–Kucera parameter Q (Section 2), and well known fundamental design trade-offs associated with such systems, e.g. compromises which have to be made between internal stability requirements, robust stability and performance specifications [12, 13]. These trade-offs may not be possible to achieve and may even result in an impossible design (Section 2.4).

To alleviate the above-mentioned concerns, two-degree-of-freedom configurations can be considered, in which a separation is made between disturbance attenuation and model referencing [14, 15]. The two degrees of freedom in configurations of this type may be parameterized in terms of two stable but otherwise free parameters Q_1 and Q_2 (Section 3).

The contribution of this paper is to propose a two-degree-of-freedom controller design method, outlined in Section 4, which inherits the model referencing feature of the IMC design method but addresses difficulties and disadvantages of the IMC (see Reference [10] and Section 2.4) in a coherent framework. Section 2 starts by stating the well-known Youla–Kucera parameterization which then leads the discussion to the distinct outlines of the IMC design method for the stable plants (Section 2.2) and for the unstable plant case (Section 2.3) to highlight some of the major difficulties of the design method in Section 2.4. Our proposed $\mathscr{H}_\infty$

design method relies on a two-degree-of-freedom scheme of Section 3 which utilizes Youla–Kucera parameterization of Section 2.1 in an elegant way to link with the work in the area of model referencing and the widely accepted $\mathscr{H}_\infty$ loop-shaping ideas of References [16, 17]. The $\mathscr{H}_\infty$ design method of Section 5 can be used for stable/unstable and SISO/MIMO systems, plants with lightly damped poles and/or zeros, plants with jω-axis zeros and can achieve a desired T_{yr} allowing control over its bandwidth even for unstable systems. The step-by-step presented design method of Section 5 offers model referencing and high performance design while ensuring a sensible robust stability margin, and relies on an $\mathscr{H}_\infty$ control problem which can be easily solved using standard software. The versatility of the proposed $\mathscr{H}_\infty$ design technique is illustrated with an example in Section 6. Section 7 contains concluding remarks.

2. BACKGROUND

2.1. Youla–Kucera parameterization

Let us consider a standard feedback arrangement shown in Figure 1 and begin with stating the well-known Youla–Kucera parameterization [1, 2] of all stabilizing controllers for a given linear time-invariant plant P.

Let $P = NM^{-1} = \tilde{M}^{-1}\tilde{N}$, with $\{M, N\}$ a right and $\{\tilde{M}, \tilde{N}\}$ a left coprime factorization of P over $\mathscr{RH}_\infty$, respectively, and let $C_0 = UV^{-1} = \tilde{V}^{-1}\tilde{U}$ be a stabilizing controller. Then every controller that internally stabilizes the feedback system in Figure 1 is parameterized by

$$C = (\tilde{V} - Q\tilde{N})^{-1}(\tilde{U} + Q\tilde{M}) \tag{1}$$

for any $Q \in \mathscr{RH}_\infty$, where $\tilde{V}$ and $\tilde{U}$ can be chosen to satisfy the Bezout identity $\tilde{U}N + \tilde{V}M = I$, see References [11, 14]. The parameterized controller C of Equation (1) can be implemented in a standard feedback structure as shown in Figure 2.

To this end, notice that the internal stability for the configuration of Figure 1 is guaranteed by ensuring $H(P, C) \in \mathscr{RH}_\infty$ [11] in the closed-loop mapping of

$$\begin{bmatrix} y \\ u \end{bmatrix} = \begin{bmatrix} P(I + CP)^{-1}C & P(I + CP)^{-1} \\ (I + CP)^{-1}C & (I + CP)^{-1} \end{bmatrix} \begin{bmatrix} r \\ d_i \end{bmatrix} = H(P, C) \begin{bmatrix} r \\ d_i \end{bmatrix} \tag{2}$$

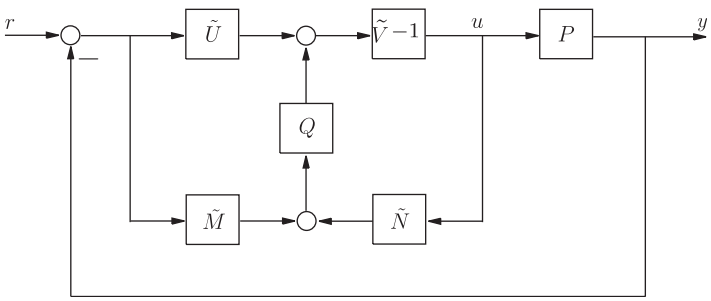

Figure 2. Youla–Kucera controller parameterization.

and one can readily verify that substituting for C in $H(P, C)$ using the parameterization of Equation (1) will result in

$$H(P,C) = \begin{bmatrix} N(\tilde{U} + Q\tilde{M}) & N(\tilde{V} - Q\tilde{N}) \\ M(\tilde{U} + Q\tilde{M}) & M(\tilde{V} - Q\tilde{N}) \end{bmatrix} \tag{3}$$

with all transfer functions evidently affine in Q.

For a model reference design, one seeks (perhaps working with the parameter Q, in Equation (3), rather than C directly) to have the transfer function T_{yr} in Figure 2 equal or otherwise reasonably close to a desired transfer function (model reference) even for MIMO/SISO, stable/unstable plants. Of course, T_{yr} is also the (1,1) block of $H(P, C)$. The IMC design methods of the following two subsections feature a model reference design, but suffer from some disadvantages discussed at the end of this section.

2.2. *Review of the IMC design scheme for stable plants*

Following the IMC design method of Reference [4], stable plants, which are simpler, are treated separately from unstable plants. For stable plants, $P \in \mathscr{RH}_\infty$, choosing $\tilde{N} = P$, $\tilde{M} = I$, $\tilde{U} = 0$ and $\tilde{V} = I$ in Equation (1) will result in the parameterization

$$C = (I - QP)^{-1}Q = Q(I - PQ)^{-1} \tag{4}$$

which is the controller parameterization exploited in the area of process control and termed IMC[‡] [4]. For $P \in \mathscr{RH}_\infty$, one can easily recover the standard IMC structure of Reference [4] in Figure 3, in which P_t denotes the true plant, from Figure 2.

It is not hard to verify that using the controller parameterization in Equation (4) and substituting for C will yield

$$H(P,C) = \begin{bmatrix} PQ & P(I - QP) \\ Q & I - QP \end{bmatrix} \in \mathscr{RH}_\infty \tag{5}$$

and clearly a resulting closed-loop transfer function, T_{yr} in Figure 1 which is linear in the free stable transfer function Q, viz. $T_{yr} = PQ$.

Recall the feedback system of Figure 1 and suppose $P \in \mathscr{RH}_\infty$ with no jω-axis zero. One decomposes P into an inner–outer factorization of the form $P = P_a P_m$ with $P_a \in \mathscr{RH}_\infty$, $P_a^{\sim} P_a = I$

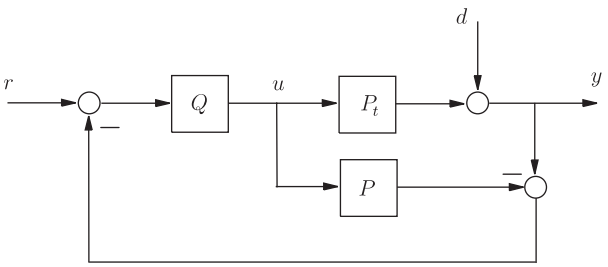

Figure 3. Standard IMC structure.

[‡] The term IMC is used because the controller can be viewed as a combination of two elements, one being a model of the plant.

and P_m stable minimum-phase (all zeros in Re[s]<0). Then the goal of obtaining a closed-loop transfer function with a desired magnitude is achieved by choosing an 'IMC filter transfer function' $F(s)$ such that with an appropriate controller, which is readily found by setting the Q-parameter in (4) to

$$Q = P_m^{-1}F \tag{6}$$

it achieves $T_{yr} = P_aF$ and hence $|T_{yr}| = |F|$. For the stable plant case, a common choice for the filter is

$$F = \left(\frac{\lambda}{s+\lambda}\right)^n \tag{7}$$

for some λ which directly specifies the desired bandwidth for T_{yr}. Evidently $Q \in \mathscr{RH}_\infty$ provided that $F \in \mathscr{RH}_\infty$ and n, the relative degree of F, is at least equal to the relative degree of P_m. Next we shall briefly outline the IMC design method of Reference [4] for unstable plants.

2.3. Review of the IMC design scheme for unstable plants

The IMC design method for unstable plants requires substantial adjustment of the stable plant scheme [4]. Let us again seek a controller parameterization for the design of C as in Equation (4) and develop the requirements on C that ensure internal stability in Figure 1. Of course, the original Youla–Kucera theory and its normal use indicate that we should use the parameterization in Equation (1). Nevertheless, for reasons of both motivation and accuracy in citing from the standard literature [4], we shall try the controller parameterization of Equation (4), undoubtedly tied with $Q \in \mathscr{RH}_\infty$, but the stability of the closed-loop system may not be guaranteed without further constraints on Q.

The closed-loop mapping of Figure 1, i.e. $\begin{bmatrix} r \\ d_i \end{bmatrix} \mapsto \begin{bmatrix} y \\ u \end{bmatrix}$ of Equation (2) and subsequently $H(P, C)$ of Equation (5) where C is substituted for as in (4), evidently indicate that to secure closed-loop stability it is necessary that: (i) $Q \in \mathscr{RH}_\infty$, (ii) the closed right half-plane poles of P must be cancelled by the zeros of Q, and (iii) the closed right half-plane poles of P must be cancelled by the zeros of $(I - QP)$. Thus, the parameterization in Equation (4) ought to be evolved to meet these constraints on Q [4]. Clearly, these interpolation constraints will complicate the design and hence we cannot expect that the choice of F as in the stable plant case together with Q as defined in Equation (6) will meet the simple requirements. All Q for which the interpolations constraints, (i)–(iii) above, are satisfied is given in Reference [4] which is in fact an alternative to the Youla–Kucera parameterization. We shall now discuss the procedure to attain a desired amplitude response for the closed-loop transfer function T_{yr} with the choice of Q and the notion of an IMC filter.

As before, and assuming that P is free of finite imaginary axis zeros, one defines $P = P_aP_m$ with P_a all-pass, with zeros restricted to Re[s] > 0, and with P_m containing all zeros in Re[s]<0, but it now may have poles in Re[s]$\geqslant 0$. Let $a_1, a_2, \ldots, a_k$ denote the closed right half-plane poles of P, assumed simple for convenience. We assert (and the reader can very easily verify) that any choice of $F \in \mathscr{RH}_\infty$ with relative degree of at least that of P and additionally such that $[P_a(s)F(s)]_{s=a_i} = 1$ will result, after retaining the choice $Q = P_m^{-1}F$ as in Equation (6), in a stabilizing controller achieving $T_{yr} = P_aF$. One then takes

$$F(s) = (b_{k-1}s^{k-1} + \cdots + b_1s + b_0)\left(\frac{\lambda}{s+\lambda}\right)^{n+k-1} \tag{8}$$

and chooses the coefficients b_i to satisfy $[P_a(s)F(s)]_{s=a_i} = 1$. One may raise the question about the implication of selecting these coefficients b_i, in the standard unstable IMC method, when the plant is not exactly known. It is discussed in Reference [4] and can be seen in the standard IMC structure of Figure 3 that for the case when $P \neq P_t$, the feedback signal expresses both the influence of (unmeasured) disturbances and the effect of model error and modifies the controller set-point accordingly. In the proposed design method of Section 5, we will 'bin' this idea and offer the choice of much simpler filters.

Clearly, the filter parameter λ, unlike the stable case (Section 2.2), no longer adjusts the bandwidth of the closed-loop frequency response. Note that b_i depend on λ, and the closed-loop bandwidth depends on the locations of the zeros of F and λ. Another approach for the choice of F is proposed in Reference [8] but it is nonetheless very application specific (e.g. excluding unstable plants with unstable zeros) and requires additional parameter tuning to trade-off the magnitude of the overshoot and the settling time in the step response.

What now follows highlights some of the major limitations and/or shortcomings of the IMC design method, applicable to *both* stable and unstable case.

2.4. *Difficulties with the IMC design method*

The discussion in Sections 2.2 and 2.3 show that the IMC design goal is achieved by setting the magnitude response of the (1,1) entry of $H(P, C)$ in Equation (2), which is the complementary sensitivity $T_{yr} = P(I + PC)^{-1}C$ and clearly important for model referencing. It only ensures that the other transfer functions in $H(P, C)$ are stable *but does not explicitly handle their sizes*. The reciprocal of the size of $\|H(P, C)\|_\infty$ is referred to as the generalized robust stability margin [18] and it corresponds to the amount of (coprime factor) uncertainty that can perturb P without destabilizing the loop [11]. Thus, we clearly wish $\|H(P, C)\|_\infty$ to be small for a robust design in this sense.

With this introduction in mind, note that the first problem arises when P has lightly damped stable poles in the closed-loop passband, for which $T_{yd_i} = P(I + PC)^{-1}$ will have large gain near the frequencies of those poles. Second is when P has lightly damped stable or unstable zeros in the closed-loop passband for which $T_{ur} = (I + PC)^{-1}C$ will have large gain near the frequencies of those zeros. This will have direct impact on the maximum singular value of $H(P, C)$, $\bar{\sigma}[H(P, C)]$, as large T_{yd_i} or large T_{ur} at some frequency means large $\bar{\sigma}[H(P, C)]$ and hence poor design. Third is when the bandwidth of F is chosen to be much larger than that of P resulting in $|C|$ being very large at frequencies inside the bandwidth of F and outside the bandwidth of P and consequently $\bar{\sigma}[H(P, C)]$ again becomes large and hence poor design.

Fourth is that the controller C becomes improper if the roll-off rate of F is desired to be less than that of P. Fifth is the fact that the simple decomposition $P = P_a P_m$ is not possible if P has zeros on the jω-axis. Sixth is when P is unstable, for which there are a series of interpolation constraints, items (i)–(iii) in Section 2.3, on the parameter Q, and direct control over the closed-loop bandwidth is not anymore possible.

The above-mentioned problems flow from an insistence on using the standard IMC structure in Figure 3 with the controller parameterization in (4) and the particular choice of $Q = P_m^{-1}F$. Thus, we shall seek a different structure and controller parameterization in order to tackle the difficulties mentioned above while maintaining the desired model referencing feature of the IMC procedure.

3. STRUCTURE ADJUSTMENT FOR IMPROVING THE IMC

In trying to address the above-mentioned difficulties and shortcomings, let us now consider the structure in Figure 4, which is a rearrangement of the controller implementation in Figure 2 but with the reference signal r entering into the structure from a different place. A similar approach in the controller implementation is utilized in Reference [19] in the area of fault-tolerant control but the closed-loop mapping is different.

The closed-loop scheme of Figure 4 offers advantages over the standard IMC approach. In this representation, Q is only required to be stable and there is no need for Q to satisfy a set of interpolation constraints discussed in Section 2.3 in order to guarantee closed-loop stability. This is because the scheme of Figure 4 reflects the full Youla–Kucera parameterization as in Equation (1) rather than that of Equation (4). Moreover, when $P_t = P$, i.e. a perfect model of the true plant is available, the structure in Figure 4 reduces to a closed-loop scheme for model reference design—where the objective is to ensure that the output of the plant follows a reference trajectory in the face of disturbances and uncertainty—which is discussed in detail in [14, 18] and is shown in Figure 5.

For the scheme of Figure 5, it is immediately seen that $y = NQr$ and hence the model reference problem is dealt with separately from the disturbance rejection problem [14] (since $\tilde{V}$ and $\tilde{U}$ deal with the disturbance rejection).

If C_0 or equivalently $\tilde{V}$ and $\tilde{U}$ are chosen simply to ensure closed-loop stability, however, the single free parameter Q in Figure 4 needs to be designed such that robustness with respect to model uncertainty, disturbance rejection, performance objectives, and robust tracking are achieved simultaneously, which may be hard to reach a trade–off [12, 13]. Thus a separation of tasks is required.

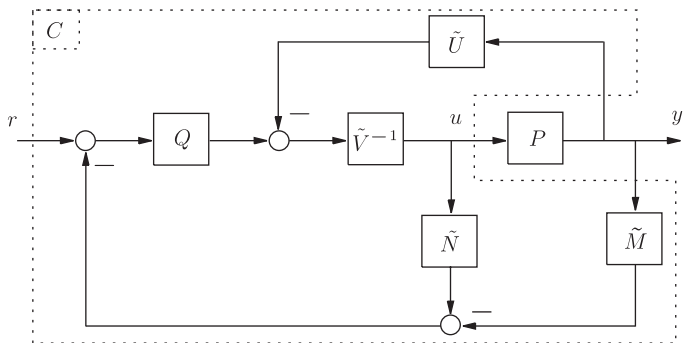

Figure 4. Youla–Kucera parameterization and IMC.

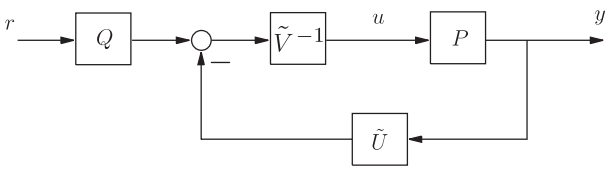

Figure 5. A model reference structure.

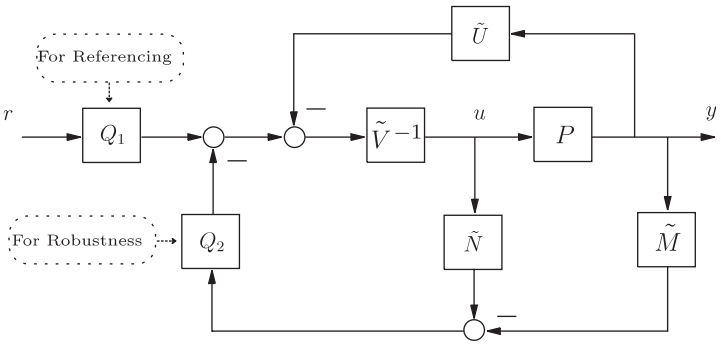

Figure 6. A two-degree-of-freedom controller structure.

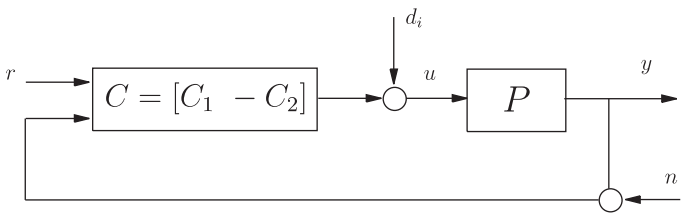

Figure 7. Standard two-degree-of-freedom structure.

The two-degree-of-freedom controller structure depicted in Figure 6 is a development of the structure discussed above and shown in Figure 4, but has more appealing properties, one being the separation of model referencing and robustness, which are discussed in the sequel. This is achieved by the use of two parameters, rather than one, both still in $\mathscr{RH}_\infty$.

In terms of the standard two-degree-of-freedom controller scheme, Figure 6 can be redrawn as Figure 7 and the set of all stabilizing controllers is given by

$$C_1 = (\tilde{V} + Q_2\tilde{N})^{-1}Q_1$$
$$C_2 = (\tilde{V} + Q_2\tilde{N})^{-1}(\tilde{U} - Q_2\tilde{M}) \tag{9}$$

for any $Q_1, Q_2 \in \mathscr{RH}_\infty$, where $\tilde{V}$ and $\tilde{U}$ are chosen to satisfy the Bezout identities $\tilde{U}N + \tilde{V}M = I$. Similar parameterizations appear in the literature [14, 19–21] using Q_1 and Q_2 but we utilize the proposed structure as it appears in this specialized way in Figure 6.

In satisfying internal stability requirements in Figure 7, one requires the mapping $\begin{bmatrix} r \\ n \\ d_i \end{bmatrix} \mapsto \begin{bmatrix} y \\ u \end{bmatrix}$ to be stable. That is to ensure

$$\Psi(P, C) = \begin{bmatrix} P \\ I \end{bmatrix}(I + C_2P)^{-1}[C \quad I] \in \mathscr{RH}_\infty \tag{10}$$

One can readily establish a link between $\Psi(P, C)$ and $H(P, C)$ of (2) by observing that $\Psi(P, C) = [\Psi_1(P, C) \quad \Psi(P, C_2)]$ with $\Psi(P, C_2) = H(P, C_2)\begin{bmatrix} -I & 0 \\ 0 & I \end{bmatrix}$, and hence $\|\Psi(P, C_2)\|_\infty = \|H(P, C_2)\|_\infty$. This link allows us to often work interchangeably with $H(P, C_2)$ and $\Psi_2(P, C_2)$ in the rest of this manuscript.

To better highlight some important advantages of considering the configuration of Figure 6, or the similar two-degree-of-freedom structure in Figure 7, substitute for $C = [C_1 \ -C_2]$ given in (9) into $\Psi(P, C)$ of (10) to yield

$$\Psi(P,C) = \begin{bmatrix} NQ_1 & -N(\tilde{U} - Q_2\tilde{M}) & N(\tilde{V} + Q_2\tilde{N}) \\ MQ_1 & -M(\tilde{U} - Q_2\tilde{M}) & M(\tilde{V} + Q_2\tilde{N}) \end{bmatrix} \tag{11}$$

Evidently, the first column of $\Psi(P, C)$, T_{yr} and T_{ur}, is affine in Q_1 and handles model reference behaviour, while the other two columns are $H(P, C_2)$ and are all affine in Q_2 and deal with the stability of feedback loop and disturbance rejection and robustness. We shall first discuss the choice of Q_1, its implications. Returning to our model reference design to have the transfer function from reference to the plant output $T_{yr} = \Psi_{11} = NQ_1$ equal or close to a desired transfer function[§] F, we need to find the free parameter Q_1 to achieve this. That is to find Q_1 which makes $\|NQ_1 - F\|_\infty$ zero or otherwise small.

Evident in the first column of Equation (11) is that any choice of Q_1 will also automatically lock the transfer function from reference to the controller output, $T_{ur} = \Psi_{21} = MQ_1$. Obviously, T_{yr} and T_{ur} are closely related and one requires MQ_1 to be somehow well behaved, e.g. not having too high bandwidth or its size not being too large, etc. If such a choice of Q_1 to make perfect model referencing is available, then one is left to deal with disturbance rejection and robustness utilizing the other free parameter Q_2.

It may however not be straightforward to choose Q_1. If the plant P has lightly damped zeros in the left half-plane and within the closed-loop passband, they will appear as lightly damped zeros of N and can result in poor design and model referencing as Q_1 will try to cancel those zeros—provided that they are not part of the model reference F—by placing poles at the exact locations and hence $T_{ur} = MQ_1$ will be large near the frequencies of those zeros undesirably. Obviously, T_{ur} is the transfer function from reference input to control signal and must be kept below a certain size for a sensible design to avoid control actuator saturation, high power consumption and high energy control action.

Note that N normally inherits all right half-plane zeros of P, and since $Q_1 \in \mathscr{RH}_\infty$, it cannot cancel them when solving $\|NQ_1 - F\|_\infty$. This observation supported by the discussion above reveals that lightly damped stable zeros must be treated in a specialized way to prevent poor design and performance.

For the choice of Q_2, or equivalently C_2, clearly the second and third columns of $\Psi(P, C)$ in Equation (11) are actually $H(P, C_2)$ and C_2 can be obtained via an $\mathscr{H}_\infty$ loop-shaping weighting scheme discussed in the sequel. This will enable us to readily deal with the problems of disturbance rejection and robustness, and also obtain a guaranteed level of robust stability and robust performance via $\|H(P, C_2)\|_\infty^{-1} = b_{P,C}$ provided that $[P, C_2]$ is stable [11, 18]. As discussed in Section 2.4, this is referred to as the generalized robust stability margin [18] and it corresponds to the amount of (coprime factor) uncertainty that can perturb P without destabilizing the loop [11]. Thus, we clearly wish not only to have all the transfer functions in $H(P, C_2)$ small or below certain size, viz. $\|H(P, C_2)\|_\infty$ small, but also to

[§] Unlike the IMC design method, we do not assume any restriction on the choice of this desired transfer function F. As we wish to have direct control over the closed-loop bandwidth—ruling out the use of filter in (8) and the associated interpolations on b_i as its bandwidth is not directly tuned by adjusting λ—a transfer function of interest would have the form of (7).

have all the transfer functions in $\Psi(P, C)$ small after ensuring that a good model referencing is obtained.

In the following section, we shall introduce a new controller design method that achieves a sensible model reference design with a guaranteed level of robust stability and robust performance.

4. BLENDING $\mathscr{H}_\infty$ DESIGN, MODEL REFERENCING AND THE IMC

To capture our objectives—viz., to achieve a closed-loop transfer function equal or otherwise close to a desired transfer function, to extend the applicability of the design method to a wider class of plants by addressing the difficulties discussed above and some other problems highlighted in Section 2.4 in a coherent framework while ensuring a guaranteed level of robust stability and robust performance—we shall introduce a new $\mathscr{H}_\infty$ controller design problem which is based on a two-degree-of-freedom structure discussed in Section 3 and has links with the $\mathscr{H}_\infty$ loop-shaping scheme of References [16, 17] in the sense of limiting the size of $H(P, C_2)$ and in part the weighting structure.

As discussed at the end of the previous section, one seeks to obtain a good model reference design and good robustness. Put another way, one needs to trade-off between keeping the size of the transfer functions in the last two columns of (11) below certain values and minimizing the error between the desired transfer function, F, and the achievable, NQ_1, for T_{yr}. This may be hard, for example, in the presence of lightly damped stable zeros in P which we discussed earlier. As hinted in the last section, the trick is to deal with these lightly damped stable poles/zeros as if they were in the right half-plane. This is elegantly done by solving a model matching problem on a shifted jω-axis. That is, one solves

$$\xi = \inf_{\hat{\Theta} \in \mathscr{RH}_\infty} \|\hat{N}\hat{\Theta} - \hat{F}\|_\infty \tag{12}$$

where $\hat{F}(s) := F(s - \alpha)$, α is the amount by which we shift the jω-axis to the left and will be discussed in Section 4.2, and $\hat{P}(s) := P(s - \alpha) = \hat{N}\hat{M}^{-1}$. Then $\Theta(s)$ is easily found to be $\Theta(s) := \hat{\Theta}(s + \alpha)$.

Then the admissible controllers $C = [C_1 \ -C_2]$ are given by solving the $\mathscr{H}_\infty$ controller design problem

$$\gamma = \inf_{C \in \underline{\mathscr{C}}} \left\| \begin{pmatrix} W_2 & 0 \\ 0 & W_1^{-1} \end{pmatrix} \times \left(\begin{bmatrix} P \\ I \end{bmatrix} (I + C_2 P)^{-1} [C_1 \ -C_2 \ I] - \begin{bmatrix} N\Theta & 0 & 0 \\ M\Theta & 0 & 0 \end{bmatrix} \right) \times \begin{pmatrix} W_3 & 0 & 0 \\ 0 & W_2^{-1} & 0 \\ 0 & 0 & W_1 \end{pmatrix} \right\|_\infty \tag{13}$$

where $N(s) := \hat{N}(s + \alpha)$ and $M(s) := \hat{M}(s + \alpha)$ and $\underline{\mathscr{C}}$ denotes the set of all proper stabilizing controllers for the plant P. Note that by solving (12) we find a Θ as a mechanism to obtain model reference transfer functions $N\Theta$ and $M\Theta$. Then the $\mathscr{H}_\infty$ problem of (13) is solved over the *entire* set of all admissible controllers C_1 and C_2, and hence they are not restricted to the parameterization (9).

The frequency weights W_1, W_2 and W_3 are stable, minimum-phase and proper weights which enforce a trade-off between achieving the model reference objectives with $\left[\begin{smallmatrix} N\Theta \\ M\Theta \end{smallmatrix}\right]$ and limiting the size of other transfer functions as will be discussed in Section 4.1. Abstractly, W_1 and W_2 are the frequency weights designed as in the standard $\mathscr{H}_\infty$ loop-shaping literature [16] and W_3 is introduced to trade-off model referencing with robust performance of the closed-loop.

The index in (13) can be rewritten as

$$\gamma = \min_{C \in \mathscr{C}} \left\| \mathscr{F}_1 \left(\left[\begin{array}{cccc} -W_2 N\Theta W_3 & 0 & W_2 P W_1 & W_2 P \\ -W_1^{-1} M\Theta W_3 & 0 & I & W_1^{-1} \\ \hdashline W_3 & 0 & 0 & 0 \\ 0 & W_2^{-1} & PW_1 & P \end{array}\right], \quad C \right) \right\|_\infty \tag{14}$$

where the term in the square bracket is usually referred to as the generalized plant and $\mathscr{F}_l(\cdot,\cdot)$ denotes the lower linear fractional transformation.

One can easily verify that the assumptions of a standard $\mathscr{H}_\infty$ control problem for the generalized plant in Equation (14) are fulfilled. The reader is referred to References [11, 22] for details on the $\mathscr{H}_\infty$ control problem and related discussions.

Note that the proposed design procedure outlined above achieves our objectives set out at the beginning of this section and can be used for stable/unstable, SISO/MIMO systems, plants with lightly damped poles and/or zeros, plants with jω-axis zeros by addressing all the difficulties discussed in Sections 2.4 and 3. Let us set down a few key points about our proposed $\mathscr{H}_\infty$ design method above.

First, we have evidently achieved the desired decomposition for P as shown above with N having all its poles to the left of the shifted axis, the $-\alpha$-axis, which ensures the stability of N with the some margin α. Likewise M is stable with the same margin α. Second, $\{\hat{N}, \hat{M}\}$ are right coprime over $\mathscr{RH}_\infty$ and hence $\left(\begin{smallmatrix} \hat{N} \\ \hat{M} \end{smallmatrix}\right)$ has full column rank for $\mathrm{Re}[s] > 0$ which in turn means that $\left(\begin{smallmatrix} N \\ M \end{smallmatrix}\right)$ not only has full column rank for $\mathrm{Re}[s] > 0$ but for the shifted open right half-plane; i.e. $\mathrm{Re}[s] > -\alpha$. Third, if ξ in (12) is small, then the norm for the unshifted model reference problem, viz. $\|N\Theta - F\|_\infty$, is even smaller by the maximum modulus theorem [11]. Fourth, if one considers the unshifted model reference problem $\inf_{\Theta \in \mathscr{RH}_\infty} \|N\Theta - F\|_\infty$, with $N\Theta$ as achievable and F as desired transfer function for T_{yr}, instead of the shifted one given in (12), problems will occur. This is because Θ, being restricted to have all its poles to the left of $-\alpha$ as $\tilde{\Theta}$, cannot cancel the lightly damped zeros in $N(s)$ as otherwise $M\Theta$ will be large at the frequencies where Θ would have been large (due to the cancellation of the zeros of N by Θ). Fifth, γ reflects a sensible measure of robust stability and robust performance and hence the problems of disturbance rejection and robustness to uncertainty are dealt with as it will become clearer shortly when the choice of W_1, W_2 and W_3 is discussed.

Sixth, a two-degree-of-freedom design method is proposed in Reference [20] in which two techniques are discussed and applied to a high purity distillation system. We shall highlight some key differences between our proposed design method and the second approach, which is more relevant in our context, of Reference [20]. (i) In Reference [20], the design of controllers C_1 and C_2 are separated. The standard McFarlane–Glover loop-shaping procedure is utilized first for the design of C_2. Then, this controller, C_2, is used and kept fixed in a separate model matching problem to find C_1. In our proposed design procedure, however, by solving model matching problem in Equation (12) one finds a Θ as a mechanism to obtain model reference

transfer functions $N\Theta$ and $M\Theta$. Then the $\mathscr{H}_\infty$ problem of (13) is solved over the *entire* set of all admissible controllers C_1 and C_2 and their designs are not separated; (ii) In our proposed $\mathscr{H}_\infty$ controller design method, the frequency weight function $W_3(s)$ is introduced as a part of the $\mathscr{H}_\infty$ index in (13) to give the designer an extra tuning knob to enable an adequate trade-off between robustness (as characterized by the size of the weighted $H(P, C_2)$) and model matching. Hence, by appropriate selection of W_3, γ also reflects how good model matching with Θ has been achieved, viz. the smaller the γ, the better the model matching achieved. This enables the establishment of a link with the results in the standard literature for adequate robustness and obtain the acceptable range for γ for a good design (Section 4.1), thereby removing *ad hoc* aspect from the design and making it easier to determine, via one number γ, when the design specifications have been fulfilled. This concurrent trade-off between achieving a sensible model matching objective and robust design is missing from the work of Limebeer *et al.* [20]; (iii) Evident in the discussion of Section 4 is the notion of shifting jω-axis for the reasons given above and specifically formulated in fourth point in the previous paragraph. The design method of Reference [20] does not take into account these problems and hence its applicability is limited as will be shown in the discussion following the numerical example in Section 6.

4.1. Choice of W_1, W_2 and W_3

Weighting functions W_1, W_2 and W_3 were introduced as a part of the $\mathscr{H}_\infty$ index in (13) to achieve the desired effect. As discussed before, we incorporate the weighting-scheme of the $\mathscr{H}_\infty$ loop-shaping design procedure proposed in Reference [16] as it has proven to be an effective method for designing robust controllers and has found its application in many control problems [17]. We shall briefly give guidelines for choosing weight functions W_1, W_2 and W_3.

Following the standard literature on $\mathscr{H}_\infty$ loop-shaping [16, 17, 23] in the context of our proposed design procedure, one chooses W_1 to have high gain in the low-frequency region (to reduce sensitivity, for example), to increase around the closed-loop bandwidth λ (to help stability by introducing phase lead and hence improving $b_{P,C}$), and to have flat low gain in the frequency region beyond 5λ. The frequency weighting function W_2 is chosen to have the shape of a low-pass filter with a bandwidth of around 5λ and unity gain in the low-frequency region (below λ). The weight W_2 should start decaying soon after the closed-loop bandwidth λ. Note that an algorithm that automatically designs weights W_1 and W_2 in the standard $\mathscr{H}_\infty$ loop-shaping context has been proposed in References [24, 25]. This algorithm may be used here to facilitate the selection of these weight functions.

Now we need to choose W_3 such that γ reflects good model referencing too, viz. the smaller γ is, the better model matching we achieve. Note that for a good design the acceptable range for γ, assuming that a perfect model matching is obtained, is $1 \leqslant \gamma \leqslant 3.3 (= 1/b_{P,C})$ [26]. Clearly, we wish to put weight on the first column of our index in (13), i.e. $\left[\begin{smallmatrix} W_2(\Psi_{11} - N\Theta)W_3 \\ W_1^{-1}(\Psi_{21} - M\Theta)W_3 \end{smallmatrix}\right]$, such that with a $\gamma \leqslant 3.3$ we obtain a good model matching. Hence, one chooses W_3 to have high gain in low frequencies below the closed-loop bandwidth and it should start decaying above the bandwidth λ. One should not choose W_3 to have very high gain at low frequencies as it will result in achieving a perfect model matching at the expense of having a non-robust design as γ becomes greater than 3.3. Neither should one choose W_3 to be zero or very small as this will result in a poor model matching but a robust ($\gamma \leqslant 3.3$) design, and hence a trade-off must be reached. The way these weights are chosen will be illustrated when we design W_1, W_2 and W_3 for the example of Section 6.

4.2. Guidelines for choosing α

We discussed earlier and based our design on the approach that we shall shift the jω-axis in order to place lightly damped stable poles and also lightly damped stable zeros to the right of the shifted axis. In this section, we shall develop a mechanism for choosing α, the amount by which we shift the jω-axis. One can choose α to be slightly smaller than the smallest real part of any lightly damped stable pole or zero, but it is required (Section 4) that the bandwidth of the filter F (if it has a $\lambda/(s+\lambda)$ form) is chosen such that $\alpha < \lambda$ to ensure stability of $\hat{F}$; viz. choose $\alpha : F(s-\alpha) \in \mathscr{RH}_\infty$.

Clearly, each pair of lightly damped poles has a characteristic equation, with its roots $s_{1,2} = -\zeta\omega_n \pm \mathrm{j}\omega_n\sqrt{1-\zeta^2}$, which is similar to that of a second-order system $G(s) = \omega_n^2/(s^2 + 2\zeta\omega_n s + \omega_n^2)$ where ω_n is the natural frequency and ζ is the damping ratio. One can readily verify that $\bar{\sigma}[G(\mathrm{j}\omega)] \leqslant (2\zeta\sqrt{1-\zeta^2})^{-1} \forall\omega$. If we consider only the lightly damped poles which make $\bar{\sigma}[G(\mathrm{j}\omega)] \geqslant 3\ \mathrm{d}B \forall\omega$, then we are looking for those with $0 \leqslant \zeta \leqslant 0.3832$.

One can extend the above discussion to consider lightly damped stable zeros of P. Note, however, that the lightly damped poles and zeros which lie in the category defined in the last paragraph have $0 \leqslant \zeta \leqslant 0.3832$ but may have a real part, $-\zeta\omega_n$ which is far into the left half-plane, i.e. outside the closed-loop bandwidth. We just include those lightly damped poles and zeros with $0 \leqslant \zeta \leqslant 0.3832$ and $\zeta\omega_n < \lambda$ and then α is chosen to be slightly bigger than the largest $\zeta\omega_n$.

5. THE PROPOSED $\mathscr{H}_\infty$ CONTROL DESIGN PROCEDURE

In this section, we shall summarize the proposed $\mathscr{H}_\infty$ control design method.

Step 1: Given $P(s)$, set α according to the rules given in Section 4.2 and define $\hat{P}(s) := P(s-\alpha)$ and then perform the factorization $\hat{P} = \hat{N}\hat{M}^{-1}$ with $\hat{N}$ and $\hat{M}$ normalized right coprime factors. Now define $N(s) := \hat{N}(s+\alpha)$ and $M(s) := \hat{M}(s+\alpha)$.

Step 2: Choose an appropriate transfer function for the filter F which represents the *desired* T_{yr} in Figure 6.

Step 3: Solve the $\mathscr{H}_\infty$ problem of Equation (12) using the solution given in Reference [27] and obtain $\hat{\Theta}$; viz. $\xi = \inf_{\hat{\Theta}\in\mathscr{RH}_\infty} \|\hat{N}\hat{\Theta} - \hat{F}\|_\infty$ where $\hat{F}(s) := F(s-\alpha)$. Then $\Theta(s) := \hat{\Theta}(s+\alpha)$.

Step 4: Design the frequency weights W_1, W_2 and W_3 according to the rules given in Section 4.1.

Step 5: Solve the $\mathscr{H}_\infty$ controller design problem given in (13) and obtain γ and the admissible controller $C = [C_1 \ -C_2]$.

Step 6: If $1 \leqslant \gamma \leqslant 3.3 (= 1/b_{P,C})$, the obtained C achieves the desired model reference objectives and ensures a sensible robust stability margin.

In Section 6, we shall use the above-stated procedure to show the effectiveness of our proposed $\mathscr{H}_\infty$ design method.

6. NUMERICAL EXAMPLE

We shall consider an example in order to illustrate the advantages of the proposed design method. Consider the following unstable plant model:

$$P = \frac{6(s^2 + 0.005s + 1)}{(s+1)(s+2)(s-3)}$$

with an unstable pole at $s = 3$ and lightly damped zeros at $s = -0.0025 \pm j1.0$, $\zeta = 0.0025$ (< 0.38) and $\omega_n = 1$ rad/s.

The discussion of Sections 2.3 and 2.4 revealed that the IMC design method for unstable plants is complicated and there are interpolation constraints on Q to be satisfied. Moreover, the desired filter transfer function cannot be simply chosen to be like that for the stable plant case (see Section 2.2). We also argued in Section 3 that if P has lightly damped stable zeros within the closed-loop passband (where the zeros are effective in the model), then T_{ur} will grow large near the frequencies of those zeros and hence the control signal in Figure 7 will be large which is undesired. We will show below that using our proposed design method one can achieve a design which was not previously possible (using the IMC design method for unstable plants discussed in Section 2.3 with the filter of (7)) or would result in an unsensible design with T_{ur} being large near the frequency of the lightly damped zeros (1 rad/s), see Section 2.4.

Following our proposed design procedure of Section 5, α is set to 0.028 and $\hat{P}(s) = P(s - 0.028)$. Let us choose $\lambda = 10$ and $F(s) = \lambda/(s + \lambda)$ which represents the desired transfer function for T_{yr} in Figure 7. Given that the lightly damped stable zero is inside the closed-loop bandwidth, it is clear that many design methods will have difficulty achieving a sensible design. For example, the IMC design method of Reference [4] will result in a T_{ur} with maximum gain of 560.69 near the frequency of the lightly damped zeros (1 rad/s).

Solving the $\mathscr{H}_\infty$ problem in (12) using the method of Reference [27] will result in

$$\Theta = \frac{50(s - 202.3)(s + 7.311)(s^2 + 1.658s + 1.373)}{(s + 6404)(s + 10)(s^2 + 0.299s + 1.003)}$$

with $\xi = 0.07$. Then the weighting functions W_1, W_2 and W_3 are designed according to the rules given in Section 4.1 and are plotted in Figure 8(a). As discussed in Section 4.1, the frequency weight function $W_1(s)$ is chosen to have high gain (~ 20 dB) in the low-frequency region (below $0.1\lambda = 1$ rad/s), to increase around the closed-loop bandwidth $\lambda = 10$ rad/s, and to have flat low gain (~ 9 dB) in the frequency region beyond $5\lambda = 50$ rad/s. The frequency weighting function W_2 is chosen to have the shape of a low-pass filter with a bandwidth of around 45 rad/s and unity gain in the low-frequency region below $\lambda = 10$ rad/s and it starts decaying soon after the closed-loop bandwidth $\lambda = 10$ rad/s. The frequency weighting function W_3 is set to have high gain in low frequencies below the closed-loop bandwidth of 10 rad/s and it starts decaying above 10 rad/s.

Solving the $\mathscr{H}_\infty$ index in (13), we find $\gamma = 1.897$ and $C = [C_1 \ -C_2]$. We employ the closed-loop controller reduction method[¶] detailed in Reference [28, Section 4.3] and assume that the Hankel singular values of the graph symbol of the controller are decreasingly ordered ($\sigma_1 > \sigma_2 > \sigma_3 > \cdots > \sigma_{24}$). We perform balanced realization and the result is truncated to retain all Hankel singular values greater than $0.01\sigma_1$. The resulting controllers after truncation are

$$C_1(s) = -10\,\frac{\prod_{i=1}^{13}(s - \hat{z}_i)}{\prod_{i=1}^{13}(s - p_i)}, \quad C_2(s) = 42.87\,\frac{\prod_{i=1}^{13}(s - \tilde{z}_i)}{\prod_{i=1}^{13}(s - p_i)}$$

with their zeros and poles given in Table I.

[¶] The procedure of References [28, pp. 137–140], while formulated for one-degree-of-freedom controller, extends to two degrees of freedom controllers through the use of an augmented plant $\left[\begin{smallmatrix} 0 \\ P \end{smallmatrix}\right]$.

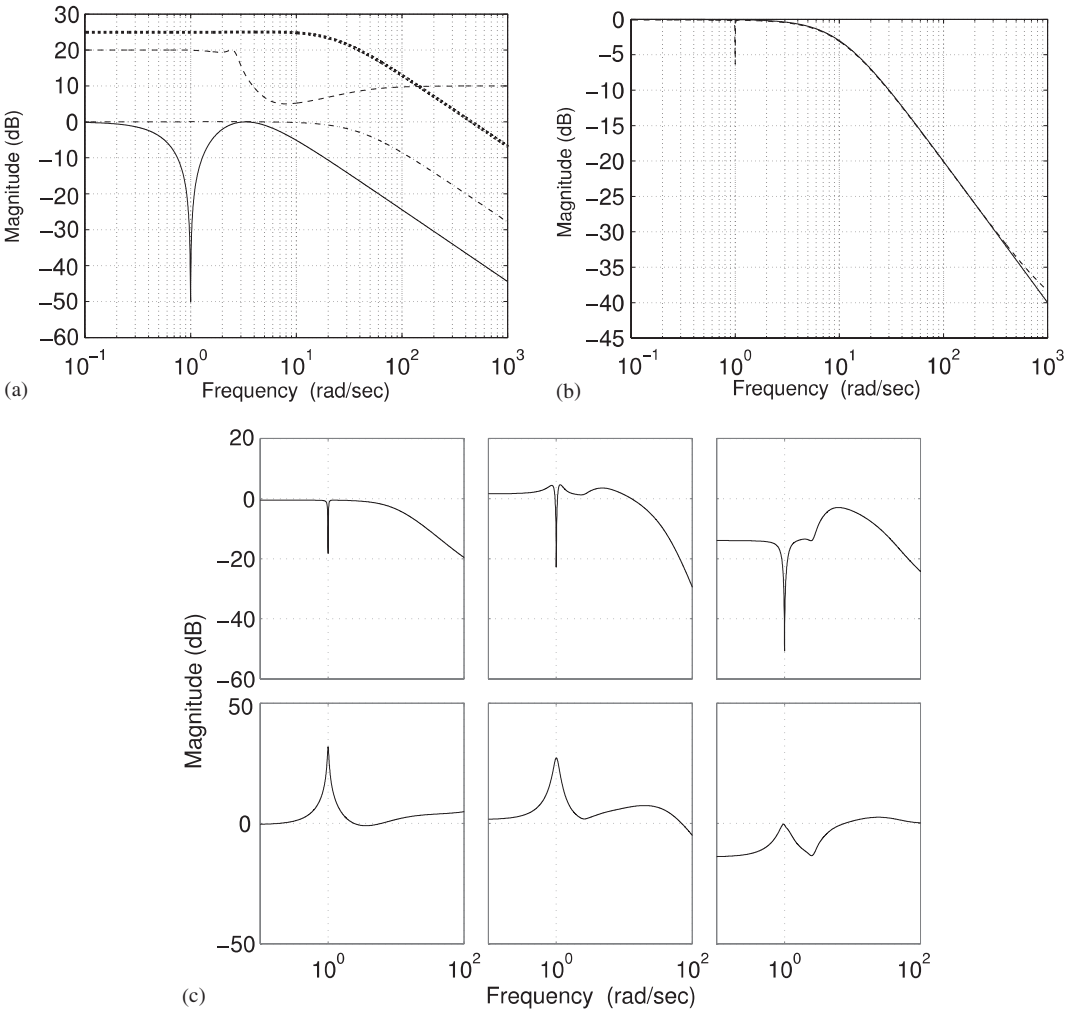

Figure 8. Magnitude responses (a) P (solid), W_1 (dash), W_2 (dash–dot), W_3 (dotted); (b) F(solid) $\Psi_{11}(P, C)$ (dashed); and (c) $\Psi(P, C)$.

Table I. Poles and zeros of $C = [C_1 \ -C_2]$.

$\hat{z}_i$	$\tilde{z}_i$	p_i
1385.9	−8498.7	−8387.4
−2.7146	−48.3	−315.46
−305.96	−12.63	−8.02
−20.978 ± j15.433	−2.70	−0.306 ± j0.42
−4.371 ± j2.814	−5.59 ± j1.69	−0.25 ± j1.007
−1.606 ± j2.690	−1.59 ± j2.42	−0.0016 ± j1.0
−0.0042 ± j1.009	−0.0064 ± j1.007	−0.002 ± j1.0
−0.0028 ± j0.999	−0.0017 ± j1.0	−20.9 ± j5.1

The frequency responses of F and Ψ_{11}, $C = [C_1 \ -C_2]$ and $\Psi(P, C)$ are plotted in Figure 8. In Figure 8(b), the magnitude response of $\Psi_{11}(P, C)$ is plotted against that of the desired transfer function F which clearly shows that a very close model matching is achieved.

Let us now record a number of key features and attributes which make the proposed two-degree-of-freedom controller design procedure of Section 5 superior to the existing design methods.

- The magnitude response of $\Psi(P, C)$ is plotted in Figure 8(c) which shows that a very good model matching on $T_{yr} = \Psi_{11}(P, C)$ is achieved and the size of T_{ur} is well contained. This has all been achieved with $\gamma = 1.897$ which shows that we have achieved a robust design too.
- The above example illustrated that one can easily use our design method for unstable plants and the filter F can have a free parameter λ directly tuning the closed-loop bandwidth as desired.
- Our proposed $\mathscr{H}_\infty$ design method provides assurance and reliability that the controller obtained meets the pre-specified performance specifications and objectives. Notice that the transfer function T_{ur} has now a reasonable maximum gain of 31.6 (it was 560.69 when the IMC design method used).
- Utilizing the two-degree-of-freedom approach in Reference [20] for the numerical example of this section, first the controller K_2 is obtained using the McFarlane–Glover loop shaping procedure with $\gamma_2 = 1.8$ which shows a robust design. However, when this controller, K_2, is used in a *separate* model matching problem to find K_1, the size of T_{ur} will be around 563 resulting in a large $\gamma_1 = 6.23$ indicating a poor design for the reasons given in Reference [20, Lemma 3.1]. Using our design method, a good design is achieved (see the first item above) with sensible robust stability and robust performance. Note that the design of $C = [C_1 \ -C_2]$ is not separated unlike the procedure of Reference [20].

7. CONCLUSIONS

We have introduced an $\mathscr{H}_\infty$ controller design method based on a proposed two-degree-of-freedom scheme which achieves a closed-loop transfer function T_{yr} equal or close to a desired transfer function F. Our proposed $\mathscr{H}_\infty$ design method generalizes the IMC design method to be used for a generic class of LTI systems. Moreover, the design method has incorporated the $\mathscr{H}_\infty$ loop-shaping ideas of Reference [16] into a two-degree-of-freedom scheme to ensure that a guaranteed level of robust stability and robust performance is obtained while achieving robust model referencing. All these have been achieved despite the existence of distinct limitations, shortcomings and restrictive assumptions detailed in Reference [10] and mentioned in Sections 2.4 and 3. These advantageous features were illustrated in Section 6.

ACKNOWLEDGEMENTS

This work was supported by an ARC Discovery-Projects Grant (DP0342683) and National ICT Australia. National ICT Australia is funded by the Australian Government's Department of Communications, Information Technology, and the Arts and the Australian Research Council through Backing Australia's Ability and the ICT Research Centre of Excellence programs.

REFERENCES

1. Kucera V. *Discrete Linear Control*: *The Polynomial Equation Approach*. Wiley: New York, 1979.
2. Youla D, Bongiorno Jr J, Jabr H. Modern Wiener–Hopf design of optimal controllers—part ii: the multivariable case. *IEEE Transactions on Automatic Control* 1976; **21**(1):319–338.
3. Zames G. Feedback and optimal sensitivity algorithm: model reference transformations, multiplicative seminorms, and approximative inverse. *IEEE Transactions on Automatic Control* 1981; **26**(2):301–320.
4. Morari M, Zafiriou E. *Robust Process Control*. Prentice-Hall: Englewood Cliffs, NJ, 1989.
5. Anderson BDO. Windsurfing approach to iterative control design. In *Iterative Identification and Control*, Albertos P, Sala A (eds). Springer: London, 2002; 143–166.
6. Lee WS, Anderson BDO, Mareels IMY, Kosut RL. On some key issues in the windsurfer approach to adaptive robust control. *Automatica* 1995; **31**:1619–1636.
7. Dehghani A, Lanzon A, Anderson BDO. An H_∞ algorithm for the windsurfer approach to adaptive robust control. *International Journal of Adaptive Control and Signal Processing* 2004; **18**(8):607–628.
8. Campi M, Lee WS, Anderson BDO. New filters for internal model control design. *International Journal of Robust and Nonlinear Control* 1994; **4**:757–775.
9. Lee WS, Mareels IMY, Anderson BDO. Iterative identification and two step control design for partially unknown unstable plants. *International Journal of Control* 2001; **74**(1):43–57.
10. Dehghani A, Lanzon A, Anderson BDO. A new H_∞ design method for high performance robust tracking control. *Proceedings of the 16th IFAC World Congress*, Prague, Czech Republic, July 2005.
11. Zhou K, Doyle JC, Glover K. *Robust and Optimal Control*. Prentice-Hall: Englewood cliffs, NJ, 1996.
12. Doyle JC, Francis BA, Tannenbaum AR. *Feedback Control Theory*. Macmillan Publishing Company: New York, 1992.
13. Goodwin GC, Graebe SF, Salgado ME. *Control System Design*. Prentice-Hall PTR: Upper Saddle River, NJ, 2000.
14. Vidyasagar M. *Control System Synthesis*: *A Factorization Approach*. The MIT Press: Cambridge, 1985.
15. Youla DC, Bongiorno Jr JJ. A feedback theory of two-degree-of-freedom optimal Wiener–Hopf design. *IEEE Transactions on Automatic Control* 1985; **30**(7):652–665.
16. McFarlane D, Glover K. A loop shaping design procedure using H_∞ synthesis. *IEEE Transactions on Automatic Control* 1992; **37**(6):759–769.
17. Papageorgiou G, Glover K. H_∞ loop shaping: why is it a sensible design procedure for designing robust flight controllers? *AIAA Conference on Guidance*, *Navigation and Control*, August 1999.
18. Vinnicombe G. *Uncertainty and Feedback*: H_∞ *Loop-shaping and the v-gap Metric*. Imperial College Press: London, 2000.
19. Zhou K, Ren Z. A new controller architecture for high performance, robust, and fault-tolerant control. *IEEE Transactions on Automatic Control* 2001; **46**(10):1613–1618.
20. Limebeer DJN, Kasenally EM, Perkins JD. On the design of robust two degree of freedom controllers. *Automatica* 1993; **29**(1):157–168.
21. Tay TT, Mareels IMY, Moore JB. *High Performance Control*. Birkhauser: Boston, 1997.
22. Green M, Limebeer DJN. *Linear Robust Control*. Prentice-Hall: Englewood Cliffs, NJ, 1995.
23. Zhou K, Doyle JC. *Essentials of Robust Control*. Prentice-Hall: Englewood Cliffs, NJ, 1998.
24. Lanzon A. Simultaneous synthesis of weights and controllers in H_∞ loop-shaping. *Proceedings of the 40th IEEE Conference on Decision and Control*, Orlando, FL, U.S.A., December 2001; 670–675.
25. Lanzon A. Weight optimisation in H_∞ loop-shaping. *Automatica* 2005; **41**(7):1201–1208.
26. Papageorgiou G, Vinnicombe G, Glover K. Guaranteed multi-loop stability margins and the gap metric. *Proceedings of the 39th IEEE Conference on Decision and Control*, vol. 4, Sydney, Australia, December 2000; 4084–4085.
27. Green M, Glover K, Limebeer D, Doyle J. A *J*-spectral factorization approach to H_∞ control. *SIAM Journal on Control and Optimization* 1990; **28**(6):1350–1371.
28. Obinata G, Anderson BDO. *Model Reduction for Control System Design*. Springer: Berlin, 2001.

